

Controlled Crystallization of Salts from Nuclear Waste Solutions – 15235

Daniel Griffin*, Martha A. Grover*, Yoshiaki Kawajiri*, Ronald W. Rousseau*

* Georgia Institute of Technology

ABSTRACT

Crystallization has been proposed as a potential method for removing low-activity salt from nuclear waste solutions. The viability of such a process hinges on the ability to partition formed salt crystals from the waste solution. Good solid-liquid separation is expected if the crystals are large and uniform, thus is important to control the crystallization operation to produce such crystals. This work examines a closed-loop control strategy for producing large salt crystals from a model electrolytic solution.

INTRODUCTION

High concentrations of sodium sulfate and other salts in nuclear waste recovered from tanks at the Hanford site can be problematic for predisposal operations such as vitrification. We are examining crystallization as a potential method for selectively removing salts—especially those containing sulfate—from nuclear waste so as to avoid complications in downstream operations. In a crystallization-separation process, solid crystals are first formed and then filtered. Separation relies on the ability to partition the solid crystals from solution, which in-turn depends on the size distribution of the formed crystals. Accordingly, the crystallization operation must be controlled to produce large, uniform crystals to achieve good separation.

Motivated primarily by applications in the pharmaceutical industry, a number of strategies have been established for controlling crystallization operations to produce crystals with the desired characteristics. However, these are typically developed for single-component systems and may not be easily applied to salt crystallization from complex multicomponent solutions of nuclear waste. From the existing crystallization control strategies, we identified two prevailing measurement-based strategies that can be applied to salt crystallizations from complex solutions. These strategies are commonly referred to as direct nucleation control (DNC) and supersaturation control (SSC) [1, 2]. In particular, for controlling salt crystallization from nuclear waste we propose the sequential application of direct nucleation control followed by supersaturation control. This strategy uses feedback from focused-beam reflectance measurements (FBRM) as well as feedback from attenuated total reflectance infrared (ATR-FTIR) absorbance measurements.

In this paper we show experimental results obtained when the proposed feedback control strategy was applied to control the crystallization of a hydrated double salt, $\text{Na}_3\text{SO}_4\text{NO}_3 \cdot \text{H}_2\text{O}$, from a model two-component electrolytic solution. Concentrations in this solution were selected to be representative of salt content in nuclear waste. Results indicate that the control scheme yields crystals that are significantly larger—and therefore easier to separate from the mother liquor—than crystals formed under simple linear cooling operations.

CRYSTALLIZATION SYSTEM, MEASUREMENTS, AND MATERIALS

This study is concerned with evaluating a feedback crystallization control strategy for producing larger more uniform crystals. To do this, we need a system capable of adjusting the operating variables (i.e. the solution temperature) according to feedback from real-time measurement and we also need a method for measuring the size of crystals produced. This section describes the crystallization system, the online measurements, and the *ex situ* techniques for measuring the crystals size distribution. In addition, details are

given for the two-component electrolytic solution used a simple model solution for high-salt content nuclear waste.

Crystallization System

Crystallization experiments were run using an OptiMax™ workstation (Fig. 1) from Mettler Toledo. This system, which provides the framework for feedback control, was integrated with two instruments for monitoring the progress of crystallization online. The first is an attenuated total reflectance Fourier-transform infrared (ATR-FTIR) measurement system, and the second a focused-beam reflectance measurement (FBRM) system. Measurements from these instruments as well as temperature measurements are recorded by iC™ software and exported in real-time to MATLAB® for processing.



Fig. 1. Optimax™ workstation equipped with focused-beam reflectance measurement (FBRM) and attenuated total-reflectance Fourier transform infrared (ATR-FTIR) online measurement technology.

Online Crystallization Monitoring

In monitoring a crystallization operation, we are interested in tracking the development of crystals as well as the evolution of the solution composition. To track the development of crystals we used focused beam reflectance measurements (FBRM). As a focused light beam scans across a solution, suspended crystals cause reflections. From the duration of reflection, the distance scanned during continuous reflection is calculated. This is termed the chord length. The number of discrete reflections—chords counts—and the distribution of chord lengths provide measures related to the number of crystals and the crystal size distribution, respectively. This principle is illustrated in Fig. 2. The FBRM equipment used in the present work is from Mettler Toledo and has a detection range of 1–1000 μm .

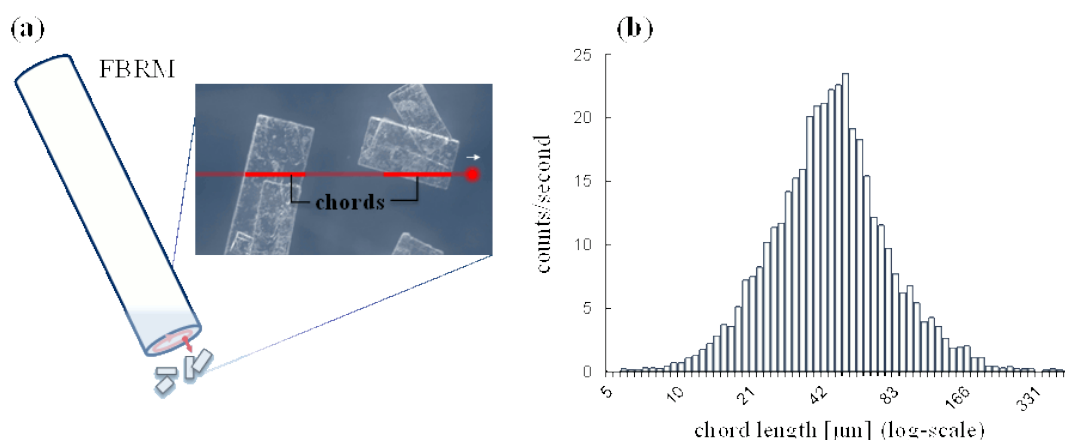


Fig. 2. (a) Focused-beam reflectance measurement (FBRM) illustration. (b) Typical chord length distribution obtained from FBRM.

To measure the evolution of the solution composition, we used attenuated total reflectance Fourier transform infrared absorbance measurements (ATR-FTIR). Different solution components absorb different frequencies of light and, furthermore, the fraction of incident light absorbed can be related to the concentration of the absorbing component. Thus, from infrared absorbance measurements, the solution composition can often be inferred. This requires a calibration model to be constructed beforehand; the calibration strategy used here follows from previously reported work [3]. Fig. 3 illustrates the ATR measurement principle and provides a typical infrared absorbance spectra to sulfate and nitrate—two key solution components in this study.

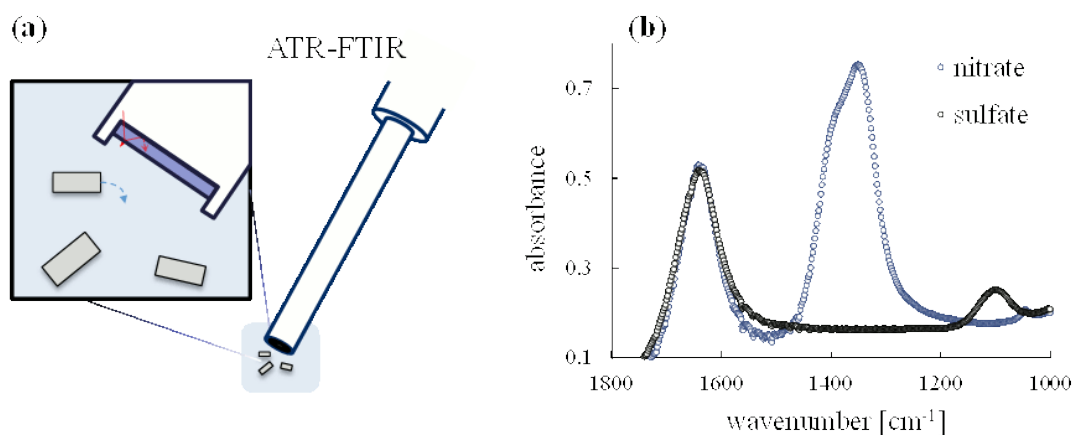


Fig. 3. (a) Attenuated total-reflectance Fourier transform infrared (ATR-FTIR) absorbance measurement illustration. (b) Typical absorbance spectrum for nitrate and sulfate in water.

Ex-situ Crystal Size Measurements

Crystals produced by the operations examined in the present work are filtered and sized. We used two different techniques for sizing the crystals. The first is sieve analysis. As illustrated in Fig. 4, this technique provides the mass of crystals of different sizes. The second technique used to size crystals is image analysis. The experimental setup we used to obtain high-contrast images of crystal samples is shown in Fig. 5. This technique provides size and shape statistics for the crystal objects identified in the image frame. To characterize the size, we used the minimum Feret's diameter. This is the minimum distance between a pair

of parallel lines tangent to the projected outline of the object and is expected to be similar to the sieve diameter of a particle [4].

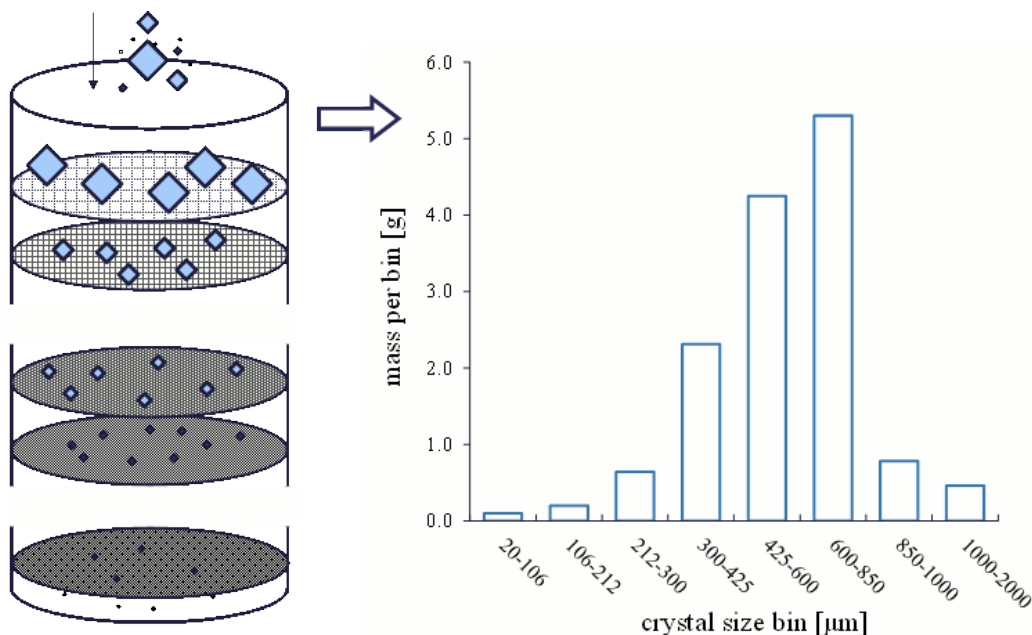


Fig. 4. Illustration of crystal size distribution estimation by sieve analysis.

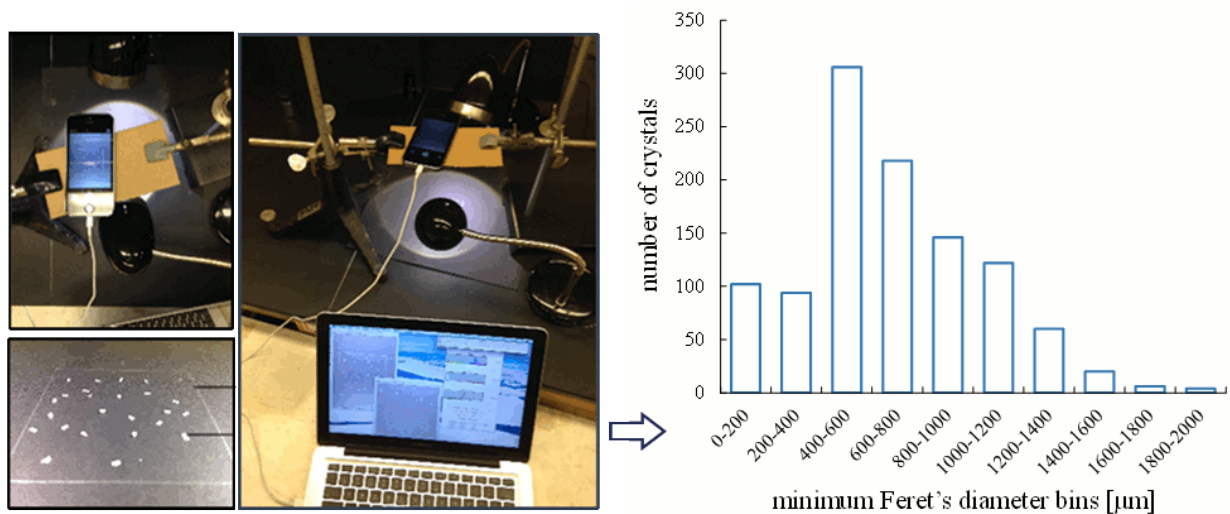


Fig. 5. Illustration of crystal size distribution estimation by image analysis.

Model Two-Component Electrolytic Solution

An aqueous solution containing sodium nitrate and sodium sulfate is used as a model solution for high-salt-content nuclear tank waste at Hanford. Sodium nitrate is chosen because it is the most abundant salt in Hanford waste; sodium sulfate is chosen because sulfate is a target component for removal. Specifically, we studied crystallizations from aqueous solutions initially containing 7.25 grams of dissociated Na_2SO_4 and 110 grams of dissociated NaNO_3 per 100 grams of water. These concentration levels are chosen to be representative of levels in Hanford tank waste [5-7]. From such solutions, the

crystallization of the hydrated double salt, $\text{Na}_3\text{SO}_4\text{NO}_3 \cdot \text{H}_2\text{O}$, is observed. We confirmed the identity of this salt by microscopic images and *ex situ* analysis. A microscopic image of $\text{Na}_3\text{SO}_4\text{NO}_3 \cdot \text{H}_2\text{O}$ salt crystals is given in Fig. 6(a). The typical infrared absorbance spectrum measured for the double salt dissolved in water is shown in Fig. 6(b).

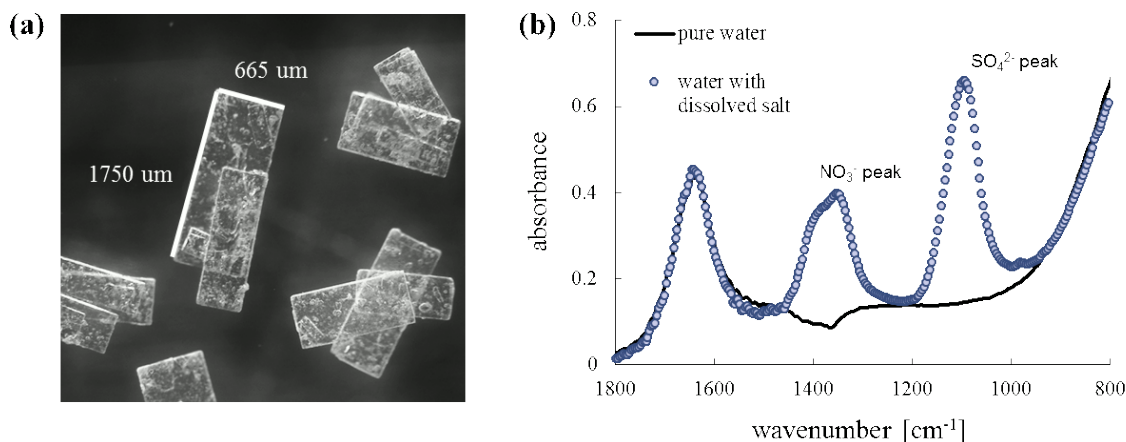


Fig. 6. (a) Optical microscope images of the double salt $\text{Na}_3\text{SO}_4\text{NO}_3 \cdot \text{H}_2\text{O}$. (b) Infrared absorbance the double salt (dissolved in water).

METHODS

We have identified two model-free feedback control policies that may be used to control the size of salt crystals formed from an electrolytic solution, provided that FBRM and ATR-FTIR measurements are available. These are termed direct nucleation control (DNC) and supersaturation control (SSC). In this section we briefly review the basic concepts behind these control schemes. In addition we discuss the sequential application of these strategies—it is this combined strategy that we have chosen to examine for controlling the size of $\text{Na}_3\text{SO}_4\text{NO}_3 \cdot \text{H}_2\text{O}$ salt crystals from the model two-component electrolytic solution.

Direct Nucleation Control (DNC)

Direct nucleation control is an operation strategy that uses feedback on the number of crystals in solution (in this study, the number of chord counts from FBRM) to institute crystallization-dissolution cycles and moderate the number of crystals produced [8, 9]. The principle behind this scheme is the following. In cooling crystallization, solution thermodynamics dictate the crystal mass that can be recovered from an operation starting from a particular composition, temperature and pressure and ending in equilibrium at a given temperature and pressure; by keeping the initial and final states fixed but varying the operational path to produce fewer crystals, larger crystals are obtained.

Supersaturation Control (SSC)

Crystallization occurs by the nucleation of new crystals or the growth of existing crystals. If growth can be favored over nucleation, larger crystals can be produced. One way to promote growth over nucleation is to control the thermodynamic driving force for crystallization throughout the operation according to the heuristic that a high driving force results in nucleation, while a moderate driving force causes crystal growth. This is the idea behind supersaturation control (SSC) [10-14]. In particular, SSC adapts the operating variables (solution temperature in this study) to maintain the crystallization driving force at a pre-selected level. Implementation requires online feedback on the thermodynamic driving force.

For single component, non-electrolytic solutions, the relative supersaturation is often used as a measure of the driving force for crystallization. Relative supersaturation is defined as follows:

$$\sigma \equiv \frac{(C - C_s(T))}{C_s(T)}$$

where C is the solution concentration of the crystallizing solute and $C_s(T)$ is the solubility concentration at the given temperature, T .

The above expression points out that composition measurements (via infrared absorbance) and *a priori* knowledge of the solubility can be used to obtain the driving force for crystallization in real time. This is then used to inform temperature adjustments. Informally, the feedback scheme is the following: if the supersaturation is too high, the temperature setpoint is increased; conversely, if the supersaturation is too low, the temperature setpoint is decreased. For multicomponent electrolytic solutions, we propose the use of a slightly different measure—termed the molar supersaturation [15]—but the feedback control strategy is the same.

Sequential Application of DNC Followed by SSC

Although both DNC and SSC have been successfully employed to a number of systems to produce larger, more uniform crystals, we note two potential drawbacks for our application. DNC typically requires multiple crystallization-dissolution cycles—increasing the batch time and reducing the efficiency—and SSC usually must be implemented from a *seeded* solution—requiring material additions. We have therefore examined the sequential application of DNC followed by SSC. In this process a single DNC crystallization-dissolution loop is used to create a moderate number of “seed” crystals. This is followed by SSC to grow those seed crystals and avoid the nucleation of new crystals.

RESULTS

The objective of this study is to understand the effect of the described feedback control policy (sequential application of DNC followed by SSC) on the size of $\text{Na}_3\text{SO}_4\text{NO}_3 \cdot \text{H}_2\text{O}$ salt crystals formed from the model two-component electrolytic solution. We have therefore implemented the proposed feedback control strategy to control crystallizations of the double salt and compared the results against simple linear cooling crystallization for the same system. Both types of operations (controlled and linear cooling crystallizations) were repeated three times. The crystals obtained from each run were filtered from solution and sized. As described earlier, the crystals are sized by sieve and image analysis. From the aggregate data from the three runs of each operation, we obtain estimates of the average size distribution (by mass and crystals number). Fig. 7 presents these estimates. From this figure, we see that the feedback control scheme results in the production of fewer fines and larger crystals, on average.

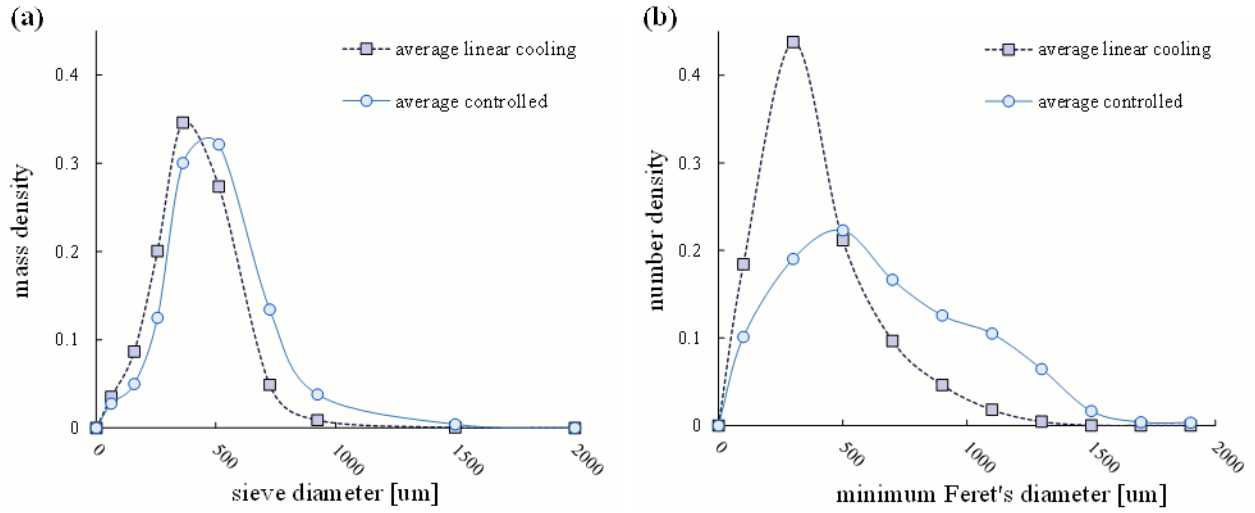


Fig. 7. (a) Average crystal size mass distributions from the three linear cooling runs and three controlled runs. (b) Average crystal size number distributions from the three linear cooling and three controlled runs.

In addition to the displayed size distributions, we quantify the effect of operating policy on the crystal size using two mean size statistics. The first is the mass-weighted mean crystal sieve diameter calculated from sieve analysis:

$$\bar{L} \equiv \frac{\sum_{i=1}^{N_{\text{bins}}} m_i L_i^{\text{mp}}}{\sum_{i=1}^{N_{\text{bins}}} m_i}$$

where m_i is the mass of crystals in the i^{th} bin, L_i^{mp} is the mid-point sieve diameter for that bin, and N_{bins} is the number of sieve bins in the stack.

The second size statistic is the average minimum Feret's diameter, calculated from image analysis data:

$$\bar{d} \equiv \frac{\sum_{j=1}^{N_{\text{obj}}} d_j^{\text{mF}}}{N_{\text{obj}}}$$

where d_j^{mF} is the minimum Feret's diameter of the j^{th} crystal object in the imaged sample and N_{obj} is the number of crystal object in the frame.

These statistics were calculated for crystals produced in each of the six runs (three linear cooling, three controlled). As shown graphically in Fig. 8, these statistics indicate that the proposed feedback control scheme results in significantly larger crystals.

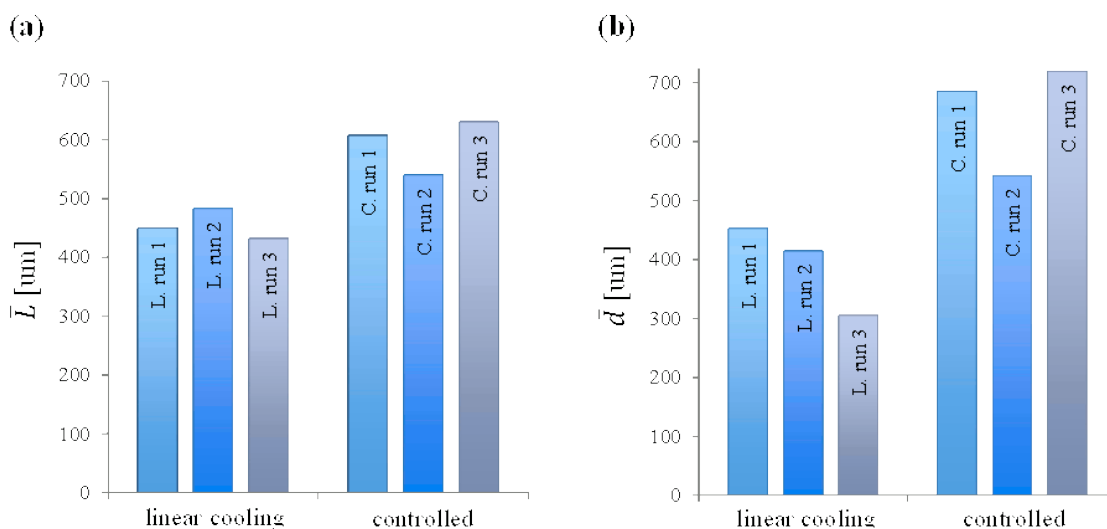


Fig. 8. (a) Mean sieve diameter of crystals from each run. (b) Mean minimum Feret's diameter of crystals from each run.

CONCLUSIONS

In this work, we have demonstrated a feedback control scheme that systematically varies the solution temperature during crystallization to produce fewer fines and larger crystals. For the model waste solution, the control scheme resulted in crystals that were 150% larger than those produced by simple, linear cooling. Such an improvement is expected to facilitate more efficient washing and improved solid-liquid separation—a critical factor in the viability of implementing a crystallization process for the separation of low activity salts from nuclear waste.

REFERENCES

1. Nagy, Z. K. and Braatz, R. D., Advances and New Directions in Crystallization Control. Annual Review of Chemical and Biomolecular Engineering, Vol. 3, 2012. 3.
2. Nagy, Z. K., Fevotte, G., Kramer, H., and Simon, L. L., Recent Advances in the Monitoring, Modelling and Control of Crystallization Systems. Chemical Engineering Research & Design, 2013. 91(10): pp. 1903-1922.
3. Griffin, D. J., Grover, M. A., Kawajiri, Y., and Rousseau, R. W., Robust Multicomponent IR-to-Concentration Model Regression. Chemical Engineering Science, 2014. 116(0): pp. 77-90.
4. Trottier, R. and Dhodapkar, S., A Guide to Characterizing Particle Size and Shape. Chemical Engineering Progress, 2014. 110(7): pp. 36-46.
5. Herting, D. L. Clean Salt Process - Final Report. 1996. Environmental Management
6. Geniesse, D. J., Nelson, E. A., Major, J. H., Nordahl, T. K., and Hamilton, D. W. Fractional Crystallization of Hanford Single-Shell Tank Wastes - From Concept to Pilot Plant. 2006. U.S. Department of Energy
7. Nassif, L., Dumont, G., Alysouri, H., and Rousseau, R. W., Pretreatment of Hanford Medium-Curie Wastes by Fractional Crystallization. Environmental Science & Technology, 2008. 42(13): pp. 4940-4945.

8. Abu Bakar, M. R., Nagy, Z. K., Saleemi, A. N., and Rielly, C. D., The Impact of Direct Nucleation Control on Crystal Size Distribution in Pharmaceutical Crystallization Processes. *Crystal Growth & Design*, 2009. 9(3).
9. Saleemi, A., Rielly, C., and Nagy, Z. K., Automated direct nucleation control for in situ dynamic fines removal in batch cooling crystallization. *Crystengcomm*, 2012. 14(6): pp. 2196-2203.
10. Feng, L. L. and Berglund, K. A., ATR-FTIR for Determining Optimal Cooling Curves for Batch Crystallization of Succinic Acid. *Crystal Growth & Design*, 2002. 2(5): p. 449-452.
11. Fujiwara, M., Chow, P. S., Ma, D. L., and Braatz, R. D., Paracetamol Crystallization Using Laser Backscattering and ATR-FTIR Apectroscopy: Metastability, Agglomeration, and Control. *Crystal Growth & Design*, 2002. 2(5): pp. 363-370.
12. Grön, H., Borissova, A., and Roberts, K. J., In-Process ATR-FTIR Spectroscopy for Closed-Loop Supersaturation Control of a Batch Crystallizer Producing Monosodium Glutamate Crystals of Defined Size. *Industrial & Engineering Chemistry Research*, 2002. 42(1): pp. 198-206.
13. Liotta, V. and Sabesan, V., Monitoring and Feedback Control of Supersaturation using ATR-FTIR to Produce an Active Pharmaceutical Ingredient of a Desired Crystal Size. *Organic Process Research & Development*, 2004. 8(3): pp. 488-494.
14. Saleemi, A. N., Rielly, C. D., and Nagy, Z. K., Comparative Investigation of Supersaturation and Automated Direct Nucleation Control of Crystal Size Distributions using ATR-UV/vis Spectroscopy and FBRM. *Crystal Growth & Design*, 2012. 12(4): pp. 1792-1807.
15. Griffin, D. J., Kawajiri, Y., Grover, M. A., and Rousseau, R. W., Sequential Application of Internal Seeding and Supersaturation Control to Salt Crystallization from a Multicomponent Solution. 2014. *Submitted*.